



**HAL**  
open science

## **X-band and Ku-band VCSEL-based optoelectronic oscillators using on-chip laser**

Juan Fernando Coronel-Rico, Christian Daniel Muñoz-Arcos, Margarita Varón-Durán, Fabien Destic, Angélique Rissons, Victor Rodrigues, Kamelya Bougueroua

► **To cite this version:**

Juan Fernando Coronel-Rico, Christian Daniel Muñoz-Arcos, Margarita Varón-Durán, Fabien Destic, Angélique Rissons, et al.. X-band and Ku-band VCSEL-based optoelectronic oscillators using on-chip laser. *Optical Engineering*, 2019, 58 (7), pp.1-4. 10.1117/1.OE.58.7.070501 . hal-02200520

**HAL Id: hal-02200520**

**<https://hal.science/hal-02200520>**

Submitted on 31 Jul 2019

**HAL** is a multi-disciplinary open access archive for the deposit and dissemination of scientific research documents, whether they are published or not. The documents may come from teaching and research institutions in France or abroad, or from public or private research centers.

L'archive ouverte pluridisciplinaire **HAL**, est destinée au dépôt et à la diffusion de documents scientifiques de niveau recherche, publiés ou non, émanant des établissements d'enseignement et de recherche français ou étrangers, des laboratoires publics ou privés.



## Open Archive Toulouse Archive Ouverte (OATAO)

OATAO is an open access repository that collects the work of some Toulouse researchers and makes it freely available over the web where possible.

This is a publisher's version published in: <https://oatao.univ-toulouse.fr/24150>

**Official URL** : <https://doi.org/10.1117/1.OE.58.7.070501>

### To cite this version :

Coronel-Rico, Juan Fernando and Muñoz-Arcos, Christian Daniel and Varón-Durán, Margarita and Destic, Fabien and Rissons, Angélique and Rodrigues, Victor and Bougueroua, Kamelya X-band and Ku-band VCSEL-based optoelectronic oscillators using on-chip laser. (2019) Optical Engineering, 58 (7). 1-4. ISSN 0091-3286

Any correspondence concerning this service should be sent to the repository administrator:

[tech-oatao@listes-diff.inp-toulouse.fr](mailto:tech-oatao@listes-diff.inp-toulouse.fr)

# Optical Engineering

OpticalEngineering.SPIEDigitalLibrary.org

## **X-band and Ku-band VCSEL-based optoelectronic oscillators using on-chip laser**

Juan Coronel  
Christian Daniel Muñoz  
Margarita Varón  
Fabien Destic  
Angélique Rissons  
Victor Rodrigues  
Kamelya Bougueroua

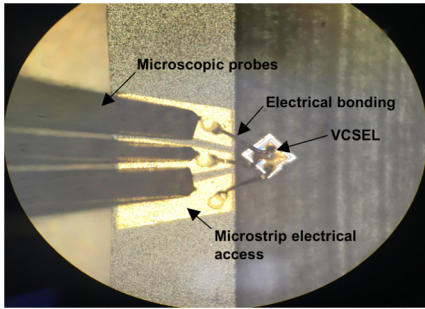


Fig. 1 Microscope view of the 850-nm VCSEL electrical connection.

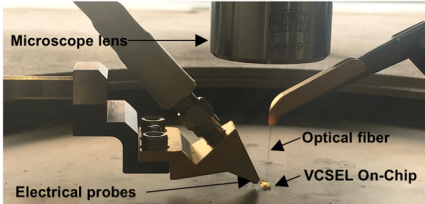


Fig. 2 On-chip 850-nm VCSEL test probe optical and electronic connection.

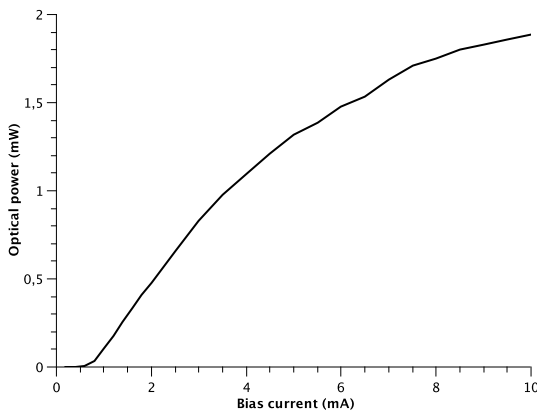


Fig. 3 On-chip 850-nm VCSEL power versus current curve.

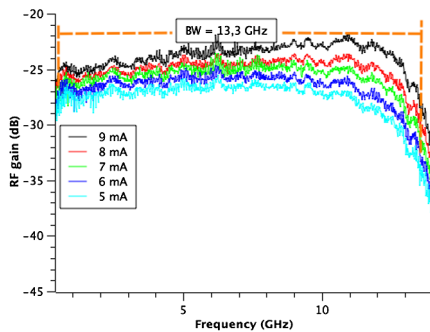


Fig. 4 On-chip 850-nm VCSEL frequency response curve.

The VCSEL is connected to a 120-m multimode optical delay line. The “delayed” light is converted into electrical domain by a Picometrix DGM-32rx high-speed photo-detector (PD). The electrical signal is amplified using a 30-dB gain wide bandwidth amplifier ( $G_{RF}$ ). The output of the amplifier is filtered using a narrow-band bandpass microwave cavity filter, tuned at the desired carrier frequency,

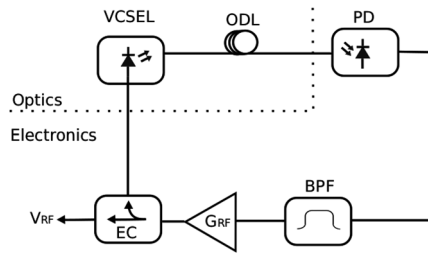


Fig. 5 Schematic setup of the VCSEL-based optoelectronic oscillator.

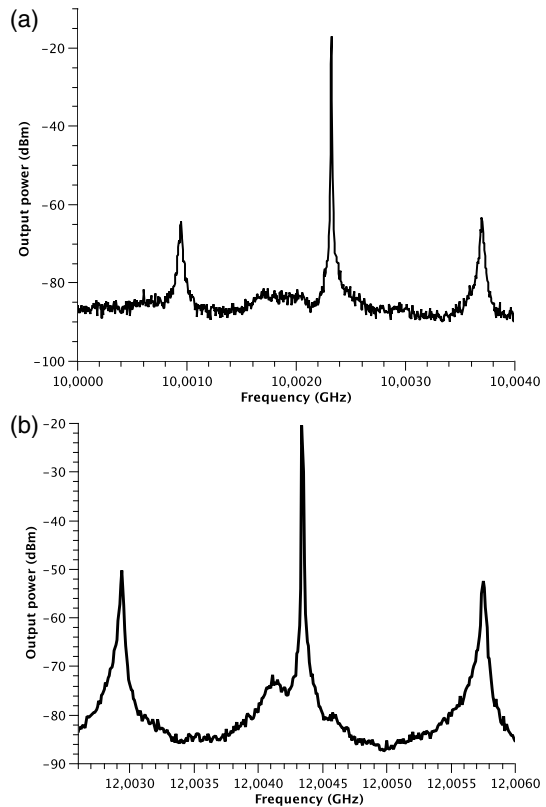
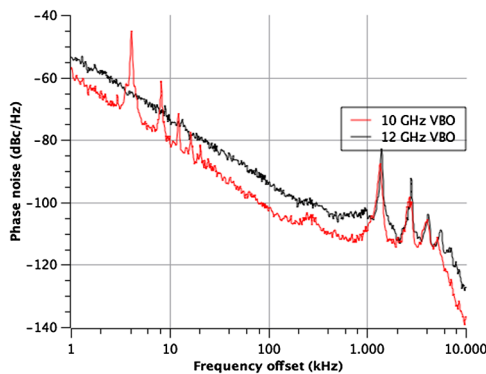


Fig. 6 Output spectrum of the VCSEL-based optoelectronic oscillator for (a) 10 GHz and (b) 12 GHz.

in order to extract an oscillation mode from the frequency comb generated, due to the delay line resonance modes. Finally, the oscillation loop is closed through a bias tee that delivers the high frequency modulation to the 850-nm on-chip VCSEL. The oscillators were implemented in a clean room controlled at 22°C and the carrier is extracted through an electrical coupler.

Figure 6 shows the implemented VBOs output spectrum at 10 GHz [Fig. 6(a)] and 12 GHz [Fig. 6(b)]. From these figures, it is possible to infer that the mode-spacing corresponds well to the oscillation modes of the 120-m optical fiber delay line. This spacing, known as free spectral range, is 1.37 MHz for the implemented oscillators. The secondary oscillations are rejected, according to the frequency response and bandwidth of each filter. The 10-GHz filter has a bandwidth of 13.93 MHz and the 12-GHz filter is 18.69 MHz, when the  $-3$ -dB band criteria is considered.

The frequency stability of the implemented VCSEL-based optoelectronic oscillators is characterized through the phase noise measurement. This measurement is performed



**Fig. 7** Phase noise curves of the implemented VCSEL-based optoelectronic oscillators.

using a Rohde & Schwarz FSW50 electrical spectrum analyzer. Figure 7 shows the phase noise curves for each oscillator. For the 10- and 12-GHz VBOs, the phase noise values at 10 kHz offset are  $-78.7$  and  $-73.8$  dBc/Hz, respectively. Table 1 presents the phase noise values for the two oscillators. These curves evidenced that the phase noise is lower for the 10-GHz VBO than for the 12-GHz VBO at the spot values. In Fig. 7, several peaks are observed for the 10-GHz VBO phase noise curve from 4.15 to 20.75 kHz. The peak at 4.15 kHz is due to the free-space interface between the VCSEL and the coupling optical fiber. This free-space produces a light reinjection into the VCSEL cavity that in turn generates a small beating mode with five harmonics observed in the curve. It is important to note that the coupling optical fiber was not exactly at the same position for both oscillators, despite the use of a micrometric positioning system.

In order to characterize the time-domain stability of the carrier, the measurement of the Allan standard deviation was performed using the VCSEL-based optoelectronic oscillator configuration. The Allan standard deviation indicates a numerical comparison of the variation of two frequency samples over a period of time. For this purpose, the measurement is performed using the FSW50 Rohde & Schwarz electrical spectrum analyzer and the software Allan variance tool downloaded from the Rohde & Schwarz website. The time-domain stability measurement is performed over a 300-s time window, and the spacing of each sample measurement is set to 0.1 s. Figure 8 shows the Allan variance curve for the 10-GHz VBO and 12-GHz VBO.

These curves allow one to infer that in the measurement range the 12-GHz VBO exhibits higher stability than the 10-GHz VBO. The time-domain stability of the oscillators is defined by several factors. The first one is the VCSEL relative intensity noise (RIN) at 10 and 12 GHz. When

**Table 1** Spot phase noise values for the implemented VCSEL-based optoelectronic oscillators.

VBO nominal frequency (GHz)	Phase noise at 10 kHz offset (dBc/Hz)	Phase noise at 100 kHz offset (dBc/Hz)	Phase noise at 1000 kHz offset (dBc/Hz)	Phase noise at 10,000 kHz offset (dBc/Hz)
10	-78.7	-102.9	-108.8	-136.8
12	-73.8	-93.5	-102.2	-127.4

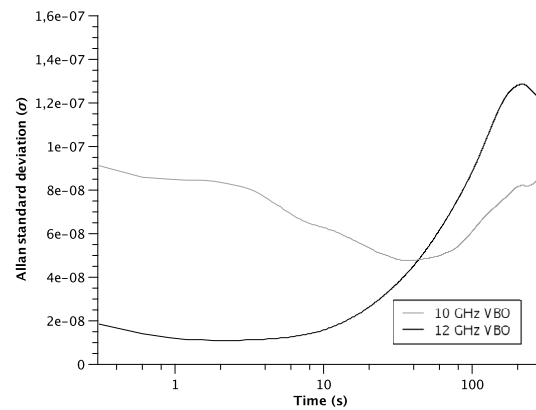


**Fig. 8** Allan standard deviation curves for the implemented VCSEL-based optoelectronic oscillators.

VCSELs are under direct modulation, they may experience higher or lower RIN values. This depends on the resonance peak of the RIN curve. If the VCSEL is modulated at RIN resonance peak, it will experience a response degradation. In addition, the optoelectronic oscillator time-domain stability is linked to the microwave amplifier used for the setup. In our experiments, different amplifiers are used for the 10- and 12-GHz OEOs, which may explain part of the stability behavior curve. However, when the two curves cross at 40 s, there is a degradation of the time-domain stability of the 12-GHz VBO while the 10-GHz VBO trend continues at the same magnitude order.

To enhance the time-domain stability of these VBOs, it is recommended to include an optical isolator at the optical fiber that collects the emitted light from the VCSEL, to avoid the reinjection phenomenon.

#### 4 Conclusions

This paper presents the results of the implementation and characterization of two VCSEL-based optoelectronic oscillators for X and Ku bands using an 850-nm on-chip VCSEL under direct modulation and without any external modulation technique. These oscillators were characterized in terms of frequency-domain stability (phase noise) and time-domain stability (Allan standard deviation). Results are relevant considering that the authors are not using any frequency multiplication technique, just a relatively simple setup with a low cost and low power consumption laser.

It is concluded that it is possible to use a direct-modulated on-chip VCSEL at frequency as high as 13.3 GHz with no need of any external modulator. The current required to bias the VCSEL is lower than 10 mA, which contrasts with the higher requirements of DFB lasers of some tens of milliamperes.

To underline the relevance of these results, Table 2 presents the reported results of several workgroups for oscillators at the same frequency bands and the technology used for the implementation. The simplicity of the implemented VBOs of this work evidences that it has a high performance when compared to the topologies of other more complex optoelectronic oscillators. The aim of this work is to obtain the best performance with the simplest technology, considering future embedded applications that require low cost and low power consumption with no frequency multiplication.

To improve its performance, it is important to consider that the optoelectronic oscillator follows the concept of

**Table 2** Performance comparison with other optoelectronic oscillator technology.

Authors	Year	Oscillator technology	Nominal frequency (GHz)	Phase noise at 10 kHz offset (dBc/Hz)	Comments
Fan et al. <sup>15</sup>	2017	Coupled dual loop—external modulation	10	−90	Two external modulators, and DFB laser.
			15		
Charalambous et al. <sup>4</sup>	2017	Recirculating delay line—external modulation	5.4	−88	External modulator, optical and electronic filter requirement. DFB laser.
Zhenghua et al. <sup>16</sup>	2016	Injection locked phase loop—external modulation	9.5	−143	External modulation and external feedback control circuit. DFB laser source.
Teng et al. <sup>17</sup>	2015	OEO frequency multiplication	18	−115.1	External cavity tunable laser and dual multiple Mach-Zender Modulator required.
Coronel et al. (This work)	2019	Single loop VBO	10	−78.7	Laser direct intensity modulation. VCSEL source (low power consumption laser).
			12	−73.8	

additive noise sources. Each component is considered a noise source. From this approach, it is necessary to find a trade-off between the electronic and optical components in order to reduce the noise contribution of each device to the total oscillator noise.<sup>18</sup> In this sense, from the optical side, the use of a low RIN laser is required, taking into account that under direct modulation the RIN is converted into phase noise.<sup>19</sup> For this reason, some authors have shown that there is a trade-off between the direct modulation response of the laser and its RIN value depending on the laser aperture. A small laser aperture leads to a lower RIN value but also to a reduced frequency response. For this reason, it is advised to use a medium-size aperture.<sup>20</sup>

On the one hand, the use of a low power laser avoids the contribution of stimulated Brillouin Raman stimulated diffusion. Considering the optical fiber propagation properties, it is suggested to use 1300-nm band in order to avoid chromatic dispersion and the use of a polarization maintaining fiber. On the other hand, to improve the optoelectronic oscillator performance from the electronic component side, it is important to use low noise components, such as low noise microwave amplifier and low noise insertion high-speed photodetector (low shot noise).<sup>21</sup>

For future work, it is important to enhance the microwave performance of the VCSEL packaging in order to avoid the use of a test probe facility and to facilitate the laser integration into the oscillator with no parasitic effect that degrades the direct modulation of the laser. The goal of achieving 5G frequency band carriers is accomplished with no need of frequency multiplication. It is a technology road that needs to be promoted for the development of better spectrum management and radio over fiber applications, such as remote carrier distribution.

**References**

1. L. Maleki, "Sources: the optoelectronic oscillator," *Nat. Photonics* **5**(12), 728–730 (2011).
2. A. Bluestone et al., "An ultra-low phase-noise 20-GHz PLL utilizing an optoelectronic voltage-controlled oscillator," *IEEE Trans. Microwave Theory Tech.* **63**(3), 1046–1052 (2015).

3. F. Jiang et al., "An optically tunable wideband optoelectronic oscillator based on a bandpass microwave photonic filter," *Opt. Express* **21**(14), 16381–16389 (2013).
4. G. Charalambous et al., "Optoelectronic recirculating delay line implementation of a high-q optoelectronic oscillator," in *Int. Top. Meeting Microwave Photonics (MWP)*, IEEE, pp. 1–4 (2017).
5. M. E. Belkin et al., "VCSEL-based processing of microwave signals," in *Int. Top. Meeting Microwave Photonics and 9th Asia-Pacific Microwave Photonics Conf.*, pp. 284–287 (2014).
6. M. Varón-durán et al., "VCSEL based oscillator for harmonic frequency generation," in *Proc. 5th Top. Meeting Optoelectron. Distance/Displacement Meas. and Appl.*, Madrid, pp. 96–101 (2006).
7. C.-H. Chang, L. Chrostowski, and C. J. Chang-Hasnain, "Parasitics and design considerations on oxide-implant VCSELs," *IEEE Photonics Technol. Lett.* **13**(12), 1274–1276 (2001).
8. A. Bacou et al., "Electrical modeling of long-wavelength VCSELs for intrinsic parameters extraction," *IEEE J. Quantum Electron.* **46**(3), 313–322 (2010).
9. Y. Ou et al., "Impedance characteristics and parasitic speed limitations of high-speed 850-nm VCSELs," *IEEE Photonics Technol. Lett.* **21**(24), 1840–1842 (2009).
10. E. K. Lau and M. C. Wu, "Enhanced modulation characteristics of optical injection-locked lasers: a tutorial," *IEEE J. Sel. Top. Quantum Electron.* **15**(3), 618–633 (2009).
11. L. Chrostowski, X. Zhao, and C. J. Chang-Hasnain, "Microwave performance of optically injection-locked VCSELs," *IEEE Trans. Microwave Theory Tech.* **54**(2), 788–796 (2006).
12. H. Sung et al., "Optoelectronic oscillators using direct-modulated semiconductor lasers under strong optical injection," *IEEE J. Quantum Electron.* **15**(3), 572–577 (2009).
13. J. Coronel, M. Varón, and A. Rissons, "Phase noise analysis of a 10-GHz optical injection-locked vertical-cavity surface-emitting laser-based optoelectronic oscillator," *Opt. Eng.* **55**(9), 090504 (2016).
14. B. Igor and B. Zdenko, "Barkhausen criterion and another necessary condition for steady state oscillations existence," in *23rd Int. Conf. Radioelektronika (RADIOELEKTRONIKA)*, pp. 151–155 (2013).
15. F. Fan et al., "Tunable optoelectronic oscillator based on coupled double loops and stimulated Brillouin scattering," in *Int. Top. Meeting Microwave Photonics (MWP)*, IEEE, pp. 1–3 (2017).
16. Z. Zhenghua et al., "An ultra-low phase noise and highly stable optoelectronic oscillator utilizing IL-PLL," *IEEE Photonics Technol. Lett.* **28**(4), 516–519 (2016).
17. Y. Teng et al., "Tunable optoelectronic oscillator with an embedded delay-line oscillator for fine steps," *Opt. Eng.* **55**(3), 031117 (2015).
18. E. Rubiola, *Phase Noise and Frequency Stability in Oscillators*, Cambridge University Press, Cambridge (2009).
19. J. L. Gimlett and N. K. Cheung, "Effects of phase-to-intensity noise conversion by multiple reflections on gigabit-per-second DFB laser transmission systems," *J. Lightwave Technol.* **7**(6), 888–895 (1989).
20. F. Tan et al., "Effect of microcavity size to the RIN and 40 Gb/s data transmission performance of high speed VCSELs," in *CLEO*, Vol. 1, OSA, Washington, DC (2015).
21. R. Boudot and E. Rubiola, "Phase noise in RF and microwave amplifiers," *IEEE Trans. Ultrason. Ferroelectr. Freq. Control* **59**(12), 2613–2624 (2012).